Title:

Intracranially-recorded ictal direct current shifts may precede high frequency oscillations in human epilepsy

Author names and affiliations:

Kyoko Kanazawa (KK)[2], Riki Matsumoto (RM)[1], Hisaji Imamura (HI)[2], Masao Matsuhashi (MM)[3], Takayuki Kikuchi (TK)[4], Takeharu Kunieda (TK)[4], Nobuhiro Mikuni (NM)[5], Susumu Miyamoto (SM)[4], Ryosuke Takahashi (RT)[2], Akio Ikeda (AI)[1]

[1]Department of Epilepsy, Movement Disorders and Physiology, Kyoto University, [2]Department of Neurology, Kyoto University, [3]Human Brain Research Center, Kyoto University, [4]Department of Neurosurgery, Kyoto University, [5]Department of Neurological Surgery, Sapporo Medical University

Contact information for the corresponding author:

Name: Akio Ikeda M.D., Ph.D.

Address: 54 Shogoin-Kawaharacho, Sakyo-ku, Kyoto-shi, Kyoto, 606-8507, Japan

Phone: +81-75-751-3772

Fax: +81-75-751-9416

E-mail: akio@kuhp.kyoto-u.ac.jp

Key words:

DC shift; high frequency oscillation; epilepsy; glioma; focal cortical dysplasia; infraslow activity

Acknowledgements:

This work was partly supported by Grants-in-Aid for Scientific Research© 20591022 from the Ministry of Education, Culture, Sports, Science and Technology of Japan (MEXT), Research Grant (22-3) for Nervous and Mental Disorders from the Ministry of Health and Welfare and the Research Grants from the Japan Epilepsy Research of Foundation.

Highlights:

· Either ictal direct current shifts or high frequency oscillations were observed in more restricted areas than conventional ictal changes.

· Both ictal direct current shifts and high frequency oscillations contributed to delineate the core of tissue generating epileptic seizures.

· Earlier occurrence of ictal direct current shifts than high frequency oscillations may suggest an active role of glia in seizure generation.

Abstract:

Objective: We assessed the temporal-spatial characteristics of ictal direct current (DC) shifts (or infraslow activity) and high frequency oscillations (HFOs) in 16 patients with intractable focal epilepsy. Methods: The underlying etiology consisted of cortical dysplasia, glioma, hippocampal sclerosis and low-grade neuroepithelial tumor in nine, four, two and one patients, respectively. The median number of analyzed seizure events was 8.0 per patient (range: 2-10). Chronic electrocorticographic recording was

performed with (1) a band-pass filter of 0.016-600 Hz (or 0.016-300 Hz) and a sampling rate of 2,000 Hz (or 1000 Hz). Results: Ictal DC shifts and a sustained form of ictal HFOs were observed in 75.0% and 50.0% of the patients, and 71.3% and 46.3% of the analyzed seizures. Visual assessment revealed that the onset of ictal DC shifts preceded that of ictal HFOs with statistical significance in 5/7 patients. The spatial extent of ictal DC shifts or HFOs was smaller than that of the conventionally-defined seizure onset zone in 9/12 patients. Conclusion: Both ictal DC shifts and HFOs might represent the core of tissue generating seizures. Significance: Early occurrence of ictal DC shifts warrants further studies to determine the role of glia (possibly mediating ictal DC shifts) in seizure generation.

Introduction:

Digital electroencephalographic (EEG) technology has enabled us to clinically record and analyze wide-band EEG in epilepsy patients undergoing surgery in the 21st century (Ikeda et al., 1996; Bragin et al., 2005; Worrell et al., 2008; Jacobs et al., 2009). EEG components lower than 1 Hz and higher than 200 Hz can be reliably recorded. While spikes and sharp waves are considered as epileptogenic markers in conventional EEG, ictal direct current (DC) shifts, or infraslow activity, and high frequency oscillations (HFOs) are also implicated as epileptogenic markers in wide-band EEG. Terminology of slow activity will be discussed later.

Ictal DC shifts or slow shifts were initially investigated in animals in 1960s (Gumnit and Takahashi, 1965; Gumnit et al., 1970), and were suggested to reflect the activity of glias and pyramidal neurons (Speckmann and Elger, 1999). Technical difficulty to eliminate artifacts, and lack of appropriate electrode material and input impedance of EEG amplifier, however, limited the recording of ictal DC shifts in humans. Ictal DC shifts were therefore largely abandoned for the following 30 years in human epilepsy research. Intracranial seizure onset had been defined with conventional frequency activity (beta, alpha, theta and delta activities), repetitive spikes, attenuation,

and high gamma activities (40-80 Hz) until 1980s.

Ictal DC shifts, however, were reappraised in human epilepsy in 1990s (Ikeda et al., 1996; Gross et al., 1999; Ikeda et al., 1999; Hughes et al., 2005; Mader et al., 2005; Thordstein et al., 2005; Rodin et al., 2006; Ikeda, 2008; Rodin et al., 2008; Rodin and Modur, 2008; Rodin et al., 2009; Ren et al., 2011; Constantino and Rodin, 2012; Rampp and Stefan, 2012; Shih et al., 2012). Ictal DC shifts were first successfully recorded in human intractable neocortical epilepsy with subdural electrodes using alternate current (AC) amplifier with large input impedance of 200 MΩ and with time constant (TC) 10 seconds, instead of DC amplifier (Ikeda et al., 1996,1999; Ikeda, 2008), and were reported as an epileptogenic marker for the first time in humans.

Ictal DC shifts were originally defined as slow potential not detected by low frequency filter (LFF) of 1.0 Hz, but detected by opening LFF to 0.016 Hz, and upward or downward phase of each slow shift lasted at least 3 seconds (Ikeda et al., 1999). In the analysis of subdural recording in 24 patients with medically refractory partial epilepsy, 23 of 24 patients (96%) showed ictal DC shifts (Ikeda, 2008). Occurrence rate was 87 (42-100)% of seizures in each patient. Ictal DC shifts were mainly negative in polarity (21/23 patients), and were recorded regardless of etiology or epilepsy type. Ictal DC shifts occasionally occurred later than conventional ictal EEG pattern or clinical

onset, which presumably reflected recruiting process in the middle of seizures. Similar findings followed, and even interictal infraslow activity is paid attention (Ren et al., 2011; Rodin et al., 2013).

HFOs were initially investigated by unit recording in animals before digital EEG technology facilitated the recording of fast activity above 50 Hz. They are clinically well recognized by intracranial electrodes as field potentials, and are studied extensively in the field of epilepsy surgery (Ochi et al., 2007; Jacobs et al., 2008). Pathological HFOs in epilepsy primarily reflect clusters of action potentials of pyramidal cells and interneurons.

HFOs are usually defined as oscillatory activities higher than 80 Hz. Generally, 80-200 Hz activities are called ripples, and 250-500 Hz fast ripples. Inhibitory mechanism by interneurons is maintained in ripples (Jefferys et al., 2012), while fast ripples reflect hypersynchronous population spikes of excitatory pyramidal cells. Fast ripples are regarded as more related to ictal epileptogenicity in animals and humans (Bragin et al., 1999a,b,2005). Fast ripples are suggested to reflect seizure onset zone more specifically in animals (Bragin et al., 1999b), and have been extensively investigated in humans (Jacobs et al., 2009).

Modur et al. analyzed ictal HFOs (>70 Hz) in six patients with neocortical

epilepsy (Modur et al., 2011). Smaller resections, restricted mainly in the cortices generating HFOs with evolution, were correlated to favorable seizure outcome.

The novel biomarkers of human epileptogenicity are now to be delineated and require further investigations. Based on the previous studies, both ictal DC shifts and HFOs seem to be useful biomarkers independently or together to detect epileptogenic zone. Their application for diagnosis and management of epilepsy is expected, namely for epilepsy surgery and seizure prediction. The relationship among ictal DC shifts, HFOs and conventional ictal EEG change, however, is yet to be elucidated. A few manuscripts including ours (Modur and Scherg, 2009; Imamura et al., 2011; Modur et al., 2012; Wu et al., 2014) or only an abstract (Erbayat Altay et al., 2011) have shown the relation between ictal DC shifts and HFOs. We previously revealed that both ictal DC shifts and HFOs were located in the same area and were useful to detect ictal onset zone (Imamura et al., 2011). As far as we know, it was also the first report which clearly showed ictal DC shifts preceded HFOs. Systematic analysis of phase-amplitude coupling of ictal HFOs and infraslow activity was previously performed, where it was not concluded that the onset of ictal infraslow activity preceded that of HFOs (Nariai et al., 2011a).

To assess clinical usefulness of ictal DC shifts and HFOs for delineating

epileptogenic zone, we analyzed and compared the two with conventional ictal pattern recorded intracranially in 16 patients with intractable partial epilepsy in terms of (1) occurrence rate, (2) relative onset time among the three activities, and (3) correlation with pathology.

With regard to the terminology, DC shifts could be recorded not only with DC amplifier, but also well with AC amplifier with long TC such as 10 seconds (Ikeda et al., 1996). It might be more precise to call them 'DC shifts' when recorded with DC amplifier. When recorded with AC amplifier with long TC, they could be simply called 'slow shifts,' 'very slow,' 'baseline shifts' or 'infraslow activity' (Rodin and Modur, 2008; Kim et al., 2009). In this manuscript, however, we shall use the term of ictal 'DC shifts' because potentials even recorded with AC amplifier with long TC of 10 seconds could contain the feature of DC shifts, and because it has been used interchangeably in the previous literatures.

Methods:

1) Patients (Figure 1 & Table 1)

We conducted an observational study on 16 patients (six females and 10 males).

They had intractable partial epilepsy, and had chronic intracranial electrode implantation for presurgical evaluation to define seizure onset zone and eloquent areas from June, 2008 to July, 2012. Two patients with chronic intracranial electrode implantation during the period were excluded because one patient had no spontaneous seizures, and the other patient only had one subclinical seizure. Age at seizure onset was 13.2±10.5 (mean±standard deviation) years old, and age at epilepsy surgery 28.9±7.6 years old. Pathological diagnosis was as follows: focal cortical dysplasia (FCD) only=9, glioma with or without FCD=4, hippocampal sclerosis (HS)=2, low grade neuroepithelial tumor=1. Patient 4 in the present manuscript was previously reported as a case report (Imamura et al., 2011). In Patient 1 and 2 (glioma without FCD), magnetic resonance imaging (MRI) showed active and partly destructive feature in the glioma lesion such as necrosis and surrounding edema. Patient 3 and 4 (glioma with FCD) had a long history of intractable epilepsy over 8-33 years. 18F-fluorodeoxyglucose-positron emission tomography was done in 15 patients. Three patients had ictal single-photon emission computed tomography imaging. Concordance of lateralization or localization of seizure focus in those non-invasive examinations was taken into account before epilepsy surgery in case conference.

2) Invasive EEG recording

Clinically available subdural (16 patients) or depth (two patients) electrodes made of platinum were used (66.1±18.3 electrodes/patient). Subdural grid or strip electrodes had the recording diameter of 2.3 mm and center-to-center inter-electrode distance of 1 cm. Grid electrodes with the recording diameter of 1.5 and 3 mm, and center-to-center inter-electrode distance of 7 mm and 5 mm were also used in one patient (Patient 7). Grid electrodes with the recording diameter of 3 mm and center-to-center inter-electrode distance of 5 mm were also used in one patient (Patient 14). Depth electrodes had a diameter of 1.5 mm, contact length of 1 mm, and center-to-center inter-electrode distance of 5 mm.

A magnetization-prepared rapid gradient echo volumetric scan was taken before surgery, and after implantation with subdural electrodes in place (Matsumoto et al., 2004). We determined electrodes by confirming its signal voids due to the property of platinum alloy in the obtained scan image after implantation, and non-linearly co-registering them to the scan image taken before implantation.

Electrocorticogram was recorded with EEG1100 (AC amplifier with input impedance of 200 ㏁, Nihon Koden, Tokyo, Japan), in the following two conditions: (1) the bandpass filter 0.016-600 Hz, sampling rate 2,000 Hz (13 patients), (2) the

bandpass filter 0.016-300 Hz, sampling rate 1,000 Hz (three patients). Those conditions were essential to record both ictal DC shifts (Ikeda et al., 1996) and HFOs (Imamura et al., 2011). Thus we could record simultaneously ictal DC shifts, HFOs and conventional ictal EEG pattern. The two system electrodes were scalp electrodes placed on the contralateral mastoid bone (Ikeda et al., 1996,1999). As we originally did in our previous studies (Ikeda et al., 1996,1999), we initially tried to reference intracranial electrodes to the scalp electrodes placed on the mastoid bone. If it fails, we tried to reference intracranial electrodes to one of the intracranial electrodes silent of all the epileptic activity. If it still fails, we referenced intracranial electrodes to the average potential of all the intracranial electrodes. In some patients, electrodes under the epicranial aponeurosis were placed. We preferentially referenced intracranial electrodes to one of the electrodes under the epicranial aponeurosis in these patients. Median recorded seizures were 17.0 (range: 2-437) times per patient during 1-2 weeks of invasive video-EEG monitoring.

Conventional ictal EEG changes were described elsewhere (Koubeissi, 2008). Briefly, they were electrical changes accompanying clinical manifestations of seizures regardless of their morphology. Early ictal patterns may take one of various morphologies, including rhythmic sinusoidal waves, irregular spike discharge, spike and

wave activity, and low voltage fast activity. Conventional ictal EEG onset was defined with the filter setting of TC 0.1 or 0.3 seconds as appropriate, and high frequency filter of 600 or 300 Hz for sampling rate of 2000 and 1000 Hz, respectively.

Seizures included for analysis were with habitual ictal semiology, and subclinical seizures but with identical conventional ictal EEG pattern to habitual seizures were also included. Semiology and conventional electrophysiological findings of habitual seizures during implantation remained primarily the same in each patient, whether or not included in the analysis. Among them, 10 consecutive full-blown seizures were analyzed in seven patients. Less than 10 seizures (4.1±2.6 seizures/patient) were analyzed in nine patients because fewer seizures occurred, or because parts of seizures were recorded with sufficient recording condition or with uniform sampling rate and TC within the same patient. Electrodes with apparent artifacts such as electromyography (EMG) and electrode movements were excluded from analysis. The analyzed seizures occurred during the period of 2.9±2.3 days.

3) Analysis of ictal DC shifts and HFOs (Figure 2, 3)

a. Ictal DC shifts were defined as sustained negative and/or positive potentials longer than 3 seconds by the previously described method (Ikeda et al., 1999) with

some modification as follows. They should be essentially better delineated with TC of 10 seconds than that of 0.1 seconds. They must be reproducible in location, waveform, duration and amplitude within each patient.

As a condition of display, ictal DC shifts were shown as EEG traces recorded by the condition as described above, with high frequency filter of 1 Hz applied. Time window was arranged as 60 seconds of duration including 30 seconds before and after the conventional ictal EEG onset. Baseline was set to the first 12 seconds of the time window. Exceptionally, Patient 4 had ictal DC shift preceding conventional ictal change by more than 18 seconds in all the 10 seizures, in which case the time window was set between -43 seconds and +17 seconds so as to include the onset of the ictal DC shift in the time window, but after the first 12 seconds of the time window for baseline.

Onset of ictal DC shifts was defined as an onset point of the beginning of the earliest negative or positive slow shifts as shown in the lower panel of Figure 2. End of ictal DC shifts was defined as an inflection point of the end of the negative or positive slow shifts as shown in the upper panel of Figure 2. Duration was defined as a time difference from the onset to the end. Amplitude was defined as the absolute value of the maximum difference between the onset and the peak of the shifts with the largest excursion from the onset.

Two electrodes with the most and the second most prominent ictal DC shifts were arbitrarily defined as so-called “core electrodes of DC shifts” in each patient. Namely, the two electrodes were delineated by 1) the earliest onset, 2) the longest duration, and 3) the largest amplitude, as listed in the order of importance. (As seizures usually contain physiological variation to a lesser degree, all the recorded seizures were not absolutely identical. In order to better delineate conspicuous findings among the seizures, we purposely chose the number of core electrodes as two rather than only one in order to avoid any misleading by variability.) All of the above findings were to be reproduced.

b. HFOs were defined by the previously described method (Imamura et al., 2011), being fast oscillatory activity faster than 100 Hz visually identified as discrete and sustained band-like power increase clearly distinct from the preictal baseline state in short time Fourier transformation analysis.

As a condition of display, spectral power was calculated in the two conditions as mentioned above; for the frequency range of 0-500 Hz with sampling rate of 2000 Hz, and 0-300 Hz with sampling rate of 1000 Hz, in 10 Hz steps for every 100 msec. Color coordinate was shown in logarithmic scale. Time window was arranged as 30 seconds of duration as preliminary inspection showed that HFO duration was generally less than

half of DC shifts. The time window was to include 15 seconds each before and after the conventional ictal EEG onset. Baseline was set to the first 6 seconds of the time window. Exceptionally, Patient 4 had HFOs preceding conventional ictal change by more than 9 seconds in all the 10 seizures, in which case the time window was set between -29 seconds and +1 seconds so as to include the onset of the HFOs in the time window, but after the first 6 seconds of the time window for baseline. Artifacts such as EMG and movements were well eliminated because they often showed distinctively wide range of activities from slow to high frequencies across the whole vertical axis, not related to the certain frequency range in the spectrogram.

Onsets of HFOs were defined as a beginning of the band-like power increase as shown in the lower panel of Figure 2. End of HFOs was defined as the cessation of the band-like power increase as shown in the upper panel of Figure 2. Duration was defined as a period from the onset to the end.

Two electrodes with the most and the second most prominent HFOs were also arbitrarily defined as so-called “core electrodes of HFOs” in each patient. Namely, the two electrodes were delineated by 1) the earliest onset, 2) the longest duration, and 3) the largest power increase, as listed in the order of importance. All of the above findings were to be reproduced.

c. Ictal DC shifts and HFOs, both of which preceded the onset of conventional ictal EEG pattern or occurred within 5 seconds after the onset, were analyzed in 15 out of 16 patients (by excluding Patient 3 who showed no conventional ictal pattern at all, as follows). Based on this criterion, there were two patients (One of 10 seizures in each of both Patient 1 and 16) with ictal DC shift onset later than 5 seconds from the conventional ictal EEG onset, and two patients (six of nine seizures in Patient 7, and two of 10 seizures in Patient 16) showed HFO onset later than 5 seconds from the conventional ictal EEG onset. Namely, 2/69 seizures (2.9%) with ictal DC shifts and 8/48 seizures (16.7%) with HFOs were out of this analysis range.

In addition, Patient 3 showed no conventional ictal EEG pattern during invasive video-EEG monitoring. The earliest EMG activity recorded from the left upper and lower extremities in his habitual seizures was defined as a clinical seizure onset, and thus it was arbitrarily substituted for conventional ictal EEG onset. This patient showed neither ictal DC shifts nor HFOs with onset later than 5 seconds from the clinical seizure onset.

Therefore finally, we adopted a total of 16 patients. Patients without ictal DC shifts and HFOs were also included in the 16 patients to analyze occurrence rate of these activities. Onset of ictal DC shifts and HFOs were compared in relation to

conventional ictal EEG pattern. Exceptionally, onset of ictal DC shifts and HFOs were compared only between these two activities in Patient3, as this patient showed no conventional ictal EEG pattern by means of intracranial electrodes.

All of those processes were made with visual inspection by a board-certified EEGer (KK), and then by one to two board-certified EEGers (HI and AI) to obtain agreement, neither the patient names nor electrode placement being informed. Exceptionally, only one of the patient's data (Patient 4) was also previously analyzed for onset of ictal DC shifts by means of linear regression line analysis (Imamura et al., 2011).

Results:

1) Ictal DC shift/HFO occurrence rates (Table 2)

Ictal DC shifts (duration 35.5±15.6 sec, absolute amplitude 903.1±462.8 μV) occurred in 12 out of 16 patients (75.0%), and in 71.3% of all the seizures analyzed of 108 times. Ictal DC shifts were mainly negative in polarity in 11 patients (91.7%), and mainly positive in polarity in 1 patient (8.3%).

Ictal DC shifts occurred in 75.0% (3/4 patients) in glioma and 77.8% (7/9 patients) in FCD patients. The two patients with HS had electrodes placed directly on

the parahippocampal gyri, but not within the hippocampi themselves. Only one of the two patients showed ictal DC shifts only in two out of 10 seizures (20.0%).

HFOs (duration 10.7±9.7 sec, frequency 193.4±80.5 Hz) occurred in eight out of 16 patients (50.0%), and in 46.3% of all the seizures analyzed of 108 times. Three (Patient3, 4, 7) out of the eight patients with HFOs showed fast ripples (≧250 Hz). The other five (Patient 5, 8, 9, 14, 15) out of the eight patients showed ripples (<250 Hz). All the eight patients with HFOs showed the decremental frequency evolution pattern (Patient 4, 5, 7, 9, 15), or the incremental pattern followed by the decremental pattern (Patient 3, 8, 14) within the range of 127.2±67.6 Hz as shown in Figure 2.

HFOs occurred in 50.0% (2/4 patients) in glioma and 44.4% (4/9 patients) in FCD patients. Only one of the two HS patients showed HFOs, and the occurrence rate was as low as 28.6%. There was no apparent difference in terms of HFO frequency among different pathologies.

One patient showed no conventional ictal EEG change at all (Patient 3), but reproducibly showed ictal DC shifts and HFOs (Figure 4). Ictal DC shifts preceded HFOs by 3.4±2.9 seconds. Two glioma patients with FCD showed ictal DC shifts and HFOs with excellent reproducibility (90.0-100.0%).

2) Time intervals among ictal DC shifts, HFOs and conventional ictal onsets (Figure 5)

Seven out of 16 patients recorded both ictal DC shifts and HFOs together within each individual seizure (Patient 3, 4, 5, 7-9, 14). All the 6 patients with conventional ictal pattern showed the earlier onset time of ictal DC shifts (-6.2±11.0 seconds) than that of HFOs (-3.5±9.1 seconds), and five patients (Patient 4, 7-9, 14) showed statistically significant difference within subjects (Patient 4, 7, 9: Student's t test, $p<0.05$. Patient 8, 14: Wilcoxon rank sum test, $p<0.05$), as shown in Figure 5. As an overall comparison of the available data in Figure 5 across the 12 patients (Patient 1, 4, 5, 7-10, 12-16) including those with only either ictal DC shifts or HFOs from the two, there was no statistical difference of onset time between ictal DC shifts and HFOs. It may suggest that absolute time difference of ictal DC shifts and HFOs to conventional onset could vary among subjects so as to obscure the tendency as shown in the direct comparison within the subjects.

3) Ictal DC shifts within white matter (Figure 6)

One patient (Patient 14) showed ictal DC shifts (duration 21.7±4.2 sec, amplitude positive 401.7±113.3 μV) with delayed onset from conventional ictal pattern

by 0.4±2.1 seconds at a depth electrode, at least one contact of which was deeply seated within the white matter in three-dimensional MRI. All the contacts of the depth electrode remained active without abundant artifact throughout the chronic intracranial electrode implantation.

HFOs were not appreciated at this electrode.

4) Localization of ictal DC shifts and HFOs (Table 3)

Among the seven patients with both ictal DC shifts and HFOs (Patient 3, 4, 5, 7-9, 14), the ratio of electrodes with both ictal DC shifts and HFOs among electrodes with at least one of the two activities were 32.9±29.1% (6.2±8.4 electrodes with both ictal DC shifts and HFOs) (Table 3).

Among all the 16 patients, 15 patients showed conventional ictal pattern except for Patient 3, as already mentioned above. Three patients (Patient 2, 6, 11) out of those 15 patients showed neither ictal DC shifts nor HFOs, but only conventional ictal change occurred. Therefore, excluding those four patients, we analyzed in 12 patients the extent of ictal DC shifts or HFOs as compared with that of conventional ictal change from the view point of the number of electrodes where those three kinds of ictal pattern were observed. At the same time, we also tried to extract the nature of core two electrodes of

ictal DC shifts or HFOs.

Eleven patients showed ictal DC shifts and the number of electrodes involved was 9.0±11.5. Two core electrodes were identifiable in all the 11 patients based on the above mentioned criteria. Ictal DC shifts were observed in more restricted area than conventional ictal change in eight patients (Patient 1, 4, 7, 9, 10, 13, 14, 16).

Seven patients showed HFOs and the number of electrodes involved was 10.4±8.4. Two core electrodes were identifiable in all the seven patients based on the above mentioned criteria. HFOs were observed in more restricted area than conventional ictal change in three patients (Patient 7-9).

Among the 12 patients, ictal DC shifts delineated more restricted area than conventional ictal change in 8 patients (66.7%), and HFOs in 3 patients (25.0%). Taking into account at least one of the localization informations (ictal DC shifts and HFOs) delineated more restricted area than conventional ictal change in higher percentage of patients (9 patients, 75.0%).

The numbers of electrodes showing conventional ictal change, ictal DC shifts and HFOs in the 12 patients were not significantly different (Friedman nonparametric analysis of variance: $p=0.112$).

5) Seizure outcome after surgery (Table 1)

Taking all the results of conventional ictal change, DC shifts, HFOs and functional mapping into account, we finally resected epileptogenic region including ictal onset zone. Clinically, complete resection of the electrodes with conventional ictal change was often not feasible as cortices at some electrodes were determined as eloquent area by functional mapping. Epileptogenic cortices as well as epileptogenic lesions were primarily resected as much as the results of functional mapping allowed. In the present study, resection was defined as incomplete when any cortices under each electrode with conventional ictal EEG change, ictal DC shifts or HFOs were not resected.

Resection of the electrodes with conventional ictal pattern was complete in seven patients (Patient 2, 5, 6, 10-12, 15), and incomplete in eight patients (Patient 1, 4, 7-9, 13, 14, 16). Resection of the electrodes with ictal DC shifts was complete in three patients (Patient 7, 10, 16), and incomplete in nine patients (Patient 1, 3-5, 8, 9, 12-14). Resection of the electrodes with HFOs was complete in two patients (Patient 3, 5), and incomplete in six patients (Patient 4, 8, 9, 14, 15). Resection of the core electrodes of ictal DC shifts were complete in six patients (Patient 3, 5, 7, 10, 13, 16), and incomplete in six patients (Patient 1, 4, 8, 9, 12, 14). Resection of the core electrodes of HFOs were

complete in three patients (Patient 3, 5, 7), and incomplete in five patients (Patient 4, 8, 9, 14, 15).

Follow-up period of the present cases was 35±14 months. Among seven patients with complete resection of the electrodes with conventional ictal pattern, six patients (Patient 2, 5, 6, 10, 12, 15) belonged to Class I (86%) and one patient (Patient 11) to others (14%) (Engel et al., 1993). In eight patients with incomplete resection, seven patients (Patient 1, 4, 7, 8, 13, 14, 16) belonged to Class I (88%) and one patient (Patient 9) belonged to others (13%). There was no significant difference between the patients with complete and incomplete resections (Pearson's chi-square test: $p=0.919$).

All the three patients with complete resection of the electrodes with ictal DC shifts (Patient 7, 10, 16) belonged to Class I (100%). In nine patients with incomplete resection, eight patients (Patient 1, 3-5, 8, 12-14) belonged to Class I (89%) and one patient (Patient 9) belonged to others (11%). There was no significant difference between the patients with complete and incomplete resections (Pearson's chi-square test: $p=0.546$).

All the six patients with complete resection of the core electrodes of ictal DC shifts belonged to Class I (100%). In six patients with incomplete resection, five patients (Patient 1, 4, 8, 12, 14) belonged to Class I (83%) and one patient (Patient 9)

belonged to others (17%). There was no significant difference between the patients with complete and incomplete resections (Pearson's chi-square test: p=0.296).

All the two patients with complete resection of the electrodes with HFOs belonged to Class I (75%). In six patients with incomplete resection, five patients (Patient 4, 7, 8, 14, 15) belonged to Class I (83%) and one patient (Patient 9) belonged to others (17%). There was no significant difference between the patients with complete and incomplete resections (Pearson's chi-square test: p=0.537).

All the three patients with complete resection of the core electrodes of HFOs belonged to Class I (100%). In five patients with incomplete resection, four patients (Patient 4, 8, 14, 15) belonged to Class I (80%) and one patient (Patient 9) belonged to others (20%). There was no significant difference between the patients with complete and incomplete resections (Pearson's chi-square test: p=0.408).

One patient (Patient 3) without conventional ictal pattern had good seizure outcome (Class I). This patient had the electrodes with ictal DC shifts and the electrodes with HFOs completely removed, including both the core electrodes of ictal DC shifts and the core electrodes of HFOs.

Ratio of resected electrodes to ones with conventional ictal pattern were 70.4±36.4% in patients with Class I outcome (Patient 1, 2, 4-8, 10, 12-16), and

69.0±73.3% in patients with outcome other than Class I (Patient 9, 11). Ratio of resected electrodes to ones with ictal DC shifts were 61.0±61.2% in patients with Class I outcome (Patient 1, 3-5, 7, 8, 10, 12-14, 16), and 44.4% in a patient with outcome other than Class I (Patient 9). Ratio of resected electrodes to ones with HFOs were 53.8±69.1% in patients with Class I outcome (Patient 3-5, 7, 8, 14, 15), and 40.0% in a patient with outcome other than Class I (Patient 9). Ratio of resected core electrodes of ictal DC shifts to ones of DC shifts were 65.0±82.3% in patients with Class I outcome (Patient 1, 3-5, 7, 8, 10, 12-14, 16), and 50.0% in a patient with outcome other than Class I (Patient 9). Ratio of resected core electrodes of HFOs to ones of HFOs were 58.3±75.3% in patients with Class I outcome (Patient 3-5, 7, 8, 14, 15), and 0% in a patient with outcome other than Class I (Patient 9).

Discussion:

a. Generator mechanisms of DC shifts and HFOs

Recent research on the pathophysiology of epilepsy elucidated the following three possible generator mechanisms of DC shifts.

1) Ictal DC shifts reflect sustained paroxysmal depolarization shift of

pyramidal cells (Ayala et al., 1970). 2) They also reflect passive sustained depolarization of glias following massive ictal neuronal firing due to increased extracellular K^+ (Kuffler et al., 1966). 3) Moreover, recent researches indicate that glias are actively involved in the generation of ictal DC shifts.

As for the above 3), glial independent role of generating paroxysmal depolarization shift has been suggested (Tian et al., 2005). Spontaneous intra-astrocytic Ca^{2+} oscillations propagate to adjacent astrocytes via gap junctions (Parri et al., 2001). Glial depolarization is amplified as they are inter-connected with gap junctions, and behave as a functional syncytium.

The active role of glias in epileptogenicity is implied in various situations of glial dysfunction such as in extracellular K^+ buffering effects around epileptic neurons (Bordey et al., 2001; Chang and Lowenstein, 2003). In rat cortical dysplasia model, Bordey et al. showed glial function to normalize extracellular K^+ is impaired during ictal period due to abnormal distribution of K^+ channels and gap junctions. In central nervous system injury model, down regulation of inwardly rectifying K^+ channels (K_{ir}), and a reduction in K_{ir} currents have been reported (MacFarlane and Sontheimer, 1997). Blood-brain barrier opening facilitates the induction of peri-infarct spreading depolarizations through impaired homeostasis of K^+ (Lapilover et al., 2012). Extravasal

albumin in the hippocampus induces rapid changes of astrocyte function, which may impair ion and transmitter homeostasis, contributing to epileptogenesis (Braganza et al., 2012). Reactive gliosis is often a prominent feature of human mesial temporal lobe epilepsy, and of most animal models of recurrent seizures, which suggests glial involvement in appearance and therapy-refractoriness of epilepsy (Benarroch, 2009). It is noteworthy that ictal DC shifts, but not HFOs, were also recorded from the white matter in the present study. All these results strengthen our hypothesis that ictal DC shifts were generated by glias.

Physiological HFOs reflect postsynaptic potentials resulting from synchronous inhibitory interneurons (Buzsaki et al., 1992; Ylinen et al., 1995). Pathological HFOs reflect bursts of pyramidal cell population spikes or action potentials (Bragin et al., 2007; Le Van Quyen and Bragin, 2007). The present study showed that the occurrence rates of ictal HFOs were lower than ictal DC shifts (HFOs 50.0%, DC shifts 75.0%). The occurrence rates of HFOs have been previously reported to be much higher 93-100% (Nariai et al., 2011b; Fujiwara et al., 2012). The potential reason for the discrepancy in the occurrence rate of ictal HFOs across the present study and others is definition of ictal HFOs differed across studies. The previous studies took into account ictal HFOs of shorter duration (<1 second). Patients in the present study were adults

(age at epilepsy surgery 28.9±7.6 years old), while patients in the above studies (Nariai et al., 2011b; Fujiwara et al., 2012) were children, and this may be also a reason for the difference in the occurrence rates of HFOs. Interictal HFOs were not analyzed in the present study, and a future study on combined analysis of ictal and interictal HFOs is warranted.

The present study showed that ictal DC shifts generally preceded HFOs. Glioma had a marginal tendency of slightly higher occurrence rate of ictal DC shifts [75% (3/4 patients)] than HFOs [50% (2/4 patients)]. Patient 2 (glioma without FCD) failed to show ictal DC shifts at all, which could be due to the aggressive behavior of glioma lesion (i.e., necrosis, surrounding edema) in this patient interfering with the generation of ictal DC shifts.

b. Is seizure from glia or from neuron?

Bower et al. recently recorded action potentials from neurons in mesial temporal structures using microelectrode arrays in seven patients with mesial temporal lobe epilepsy (Bower et al., 2012). Only 7.6% of microelectrodes showed increased firing rates before seizure onset and only 32.4% of microelectrodes showed any seizure-related activities. They suggest that the “epileptic ensemble or network”

responsible for seizure generation are more complex and heterogeneous than previously thought.

Glias as functional syncytium may play a key role in seizure ignition. Dysfunctional gap junctions in glias play an important role in the generation of acute symptomatic seizures as discussed above. Transient albumin application to the hippocampus has been shown to entail an acute decrease in astrocyte gap junction coupling, which only recovers afterwards (Braganza et al., 2012). Blood-brain barrier dysfunction alters extracellular homeostasis, and activity-dependent increase in extracellular K^+ concentration reaches a threshold for epileptiform discharges, which further increases extracellular K^+ concentration, leading to spreading depolarizations (Lapilover et al., 2012). Therefore, glias may bridge the large gap of development from the abundant, microelectrode-recorded seizures to clinical seizures in humans. Glias could facilitate microelectrode-recorded seizures, and subsequently initiate clinical seizures.

c. Methodological aspect

Slow potential recording with AC amplifier is well achieved with low frequency filter 0.016 Hz (=TC 10 seconds). Input impedance should be higher than 50

MΩ. Although reversible electrodes more suitable, platinum electrodes are used in intracranial recording due to the toxicity of silver-silver chloride electrodes. Electrodes with larger recording surface are more suitable for slow potential recording.

Diameter of subdural electrodes is presently 2.3 mm, while it used to be 3.0 mm in early 1990's (Ikeda et al., 1996,1999). Ictal DC shifts and HFOs are well recorded with the currently employed recording surface. Ictal DC shifts and HFOs are also recorded from depth electrodes presently used, recording surface of which are generally equivalent to the subdural electrodes currently employed. Moreover, it was already shown that ictal DC shifts were also well recorded even with stainless steel (Ikeda et al., 1999). Therefore, both ictal DC shifts and HFOs are expected to be well recorded also with depth electrodes and stainless steel electrodes, if certain recording conditions are met (Ikeda et al., 1999).

Recording and analysis of ictal DC shifts and HFOs are not labor- and storage-intensive as one may expect. Ictal DC shifts can be recorded easily using AC amplifiers, and may provide useful information to complement conventional EEG findings. HFOs can be reasonably analyzed using spectrogram. Our method using wide-band EEG may help facilitate localization of the epileptogenic zone in refractory partial epilepsy.

It would be technically difficult to delineate precisely in which order ictal DC shifts, HFOs or conventional ictal patterns occur when we place intracranial electrodes relatively far from the 'real' ictal onset zone. Besides, initiation of neuronal and glial activities in seizures depend on how wide cortices (or how many cells) are involved, and how synchronously cells behave. For this purpose, microwire recording would be superior to clinical macroelectrode.

d. Seizure outcome after surgery

In the analysis of subdural recording in 24 patients with medically refractory partial epilepsy, ictal DC shifts were more restrictedly localized (1-2 electrodes) than conventional ictal EEG pattern, and could clinically aid in delineating ictal onset zone before surgery presumably as the core of tissue generating epileptic seizures (Ikeda, 2008). In regards of HFOs, although specificity of ictal HFOs still remains to be solved, interictal HFOs have been previously shown to represent a marker for seizure onset zone independent of the underlying pathology (Jacobs et al., 2009).

In the present study, seizure outcome after surgery was essentially good, and only two of 16 patients belonged to other than Class I. This is most likely the reason why it did not show significant difference whether electrodes with conventional ictal

change, ictal DC shifts and HFOs, nor the core electrodes of ictal DC shifts and HFOs were completely resected or not. The small size of the cohort (16 patients) may also be a reason for the lack of significant difference.

Seven of eight patients with incomplete resection of the electrodes with conventional ictal change (Patient 1, 4, 7, 8, 13, 14, 16) had good seizure outcome (Class I). This implies that even the extent of the resection of the electrodes with conventional ictal change may not be a sufficient indicator for seizure outcome, and further study is needed to elucidate if there is indeed ‘core epileptogenic area’.

In the present study, most of the patients became seizure-free after resection of area generating ictal DC shifts and HFOs, and it is most likely that epileptogenic zones were located at or very close to the areas with the ictal DC shifts and HFOs. No conventional ictal change was recorded in Patient 3. The mass lesion was atrophic, and had a cavity within due to adjacent arterio-venous shunt. Neuronal population was presumably not large enough to generate conventional ictal change, or subdural electrodes over the lesion may not have contacted well with the cortex due to the atrophic nature of the lesion.

One may certainly have a concern on the inclusion of Patient 3 in the present study, as the patient did not show conventional ictal EEG pattern. In this patient, the

cortices under the electrodes with ictal DC shifts and HFOs were resected, resulting in Engel Class IA We finally decided to include the patient in our cohort as we thought that it was important to describe the phenomenon that ictal DC shifts and HFOs were recorded with very good reproducibility (ictal DC shifts: 100%, HFOs: 90%) when ictal conventional EEG pattern was not recorded.

In conclusion, both ictal DC shifts and HFOs contributed to delineate the core of tissue generating epileptic seizures in human intractable epilepsy. Earlier occurrence of ictal DC shifts than HFOs suggests an active role of glia in seizure generation. A marginal tendency of ictal DC shifts and HFOs to occur in glioma with FCD may reflect increased pyramidal cell excitability due to impaired buffering mechanism of dysfunctional glias.

References:

Ayala GF, Matsumoto H, Gumnit RJ. Excitability changes and inhibitory mechanisms in neocortical neurons during seizures. J Neurophysiol 1970;33:73-85.

Benarroch EE. Astrocyte-neuron interactions: implications for epilepsy. Neurology

2009;73:1323-1327.

Bordey A, Lyons SA, Hablitz JJ, Sontheimer H. Electrophysiological characteristics of reactive astrocytes in experimental cortical dysplasia. J Neurophysiol 2001;85:1719-1731.

Bower MR, Stead M, Meyer FB, Marsh WR, Worrell GA. Spatiotemporal neuronal correlates of seizure generation in focal epilepsy. Epilepsia 2012;53:807-816.

Braganza O, Bedner P, Huttmann K, von Staden E, Friedman A, Seifert G, et al. Albumin is taken up by hippocampal NG2 cells and astrocytes and decreases gap junction coupling. Epilepsia 2012;53:1898-1906.

Bragin A, Engel J, Jr., Wilson CL, Fried I, Buzsaki G. High-frequency oscillations in human brain. Hippocampus 1999a;9:137-142.

Bragin A, Engel J, Jr., Wilson CL, Fried I, Mathern GW. Hippocampal and entorhinal cortex high-frequency oscillations (100--500 Hz) in human epileptic brain and in kainic acid--treated rats with chronic seizures. Epilepsia 1999b;40:127-137.

Bragin A, Wilson CL, Fields T, Fried I, Engel J, Jr. Analysis of seizure onset on the basis of wideband EEG recordings. Epilepsia 2005;46 Suppl 5:59-63.

Bragin A, Wilson CL, Engel J, Jr. Voltage depth profiles of high-frequency oscillations after kainic acid-induced status epilepticus. Epilepsia 2007;48 (Suppl 5):S35-40.

Buzsaki G, Horvath Z, Urioste R, Hetke J, Wise K. High-frequency network oscillation in the hippocampus. Science 1992;256:1025-1027.

Chang BS, Lowenstein DH. Epilepsy. N Engl J Med 2003;349:1257-1266.

Constantino T, Rodin E. Peri-ictal and interictal, intracranial infraslow activity. J Clin Neurophysiol 2012;29:298-308.

Engel JJ, Van Ness P, Rasmussen T. With respect to epileptic seizures. In: Engel JJ, editor. Surgical treatment of the epilepsies. 2nd ed. New York: Raven Press Ltd, 1993:609-621.

Erbayat Altay E, Bek S, Alexopoulow A, Bulacia A, Vaughn K, Burgess R. A comparison of infraslow potensials (ISP) and high frequency oscillations (HFO) from subdural recordings at the time of seizure onset. Abstract of 65th Annual Meeting of the American Epilepsy Society, 2011.

Fujiwara H, Greiner HM, Lee KH, Holland-Bouley KD, Seo JH, Arthur T, et al. Resection of ictal high-frequency oscillations leads to favorable surgical outcome in pediatric epilepsy. Epilepsia 2012;53:1607-1617.

Gross DW, Gotman J, Quesney LF, Dubeau F, Olivier A. Intracranial EEG with very low frequency activity fails to demonstrate an advantage over conventional recordings. Epilepsia 1999;40:891-898.

Gumnit RJ, Takahashi T. Changes in direct current activity during experimental focal seizures. Electroencephalogr Clin Neurophysiol 1965;19:63-74.

Gumnit RJ, Matsumoto H, Vasconetto C. DC activity in the depth of an experimental epileptic focus. Electroencephalogr Clin Neurophysiol 1970;28:333-339.

Hughes JR, Fino JJ, Patel K. A newly described ictal pattern: the initial ictal slow shift. Clin EEG Neurosci 2005;36:161-170.

Ikeda A, Terada K, Mikuni N, Burgess RC, Comair Y, Taki W, et al. Subdural recording of ictal DC shifts in neocortical seizures in humans. Epilepsia 1996;37:662-674.

Ikeda A, Taki W, Kunieda T, Terada K, Mikuni N, Nagamine T, et al. Focal ictal direct current shifts in human epilepsy as studied by subdural and scalp recording. Brain 1999;122:827-838.

Ikeda A. DC recordings to localize the ictal onset zone. In: Lüders H, editor. Textbook of Epilepsy Surgery. London: Informa, 2008:659-666.

Imamura H, Matsumoto R, Inouchi M, Matsuhashi M, Mikuni N, Takahashi R, et al. Ictal wideband ECoG: direct comparison between ictal slow shifts and high frequency oscillations. Clin Neurophysiol 2011;122:1500-1504.

Jacobs J, LeVan P, Chander R, Hall J, Dubeau F, Gotman J. Interictal high-frequency oscillations (80-500 Hz) are an indicator of seizure onset areas independent of spikes in

the human epileptic brain. Epilepsia 2008;49:1893-1907.

Jacobs J, Levan P, Chatillon CE, Olivier A, Dubeau F, Gotman J. High frequency oscillations in intracranial EEGs mark epileptogenicity rather than lesion type. Brain 2009;132:1022-1037.

Jefferys JG, Menendez de la Prida L, Wendling F, Bragin A, Avoli M, Timofeev I, et al. Mechanisms of physiological and epileptic HFO generation. Prog Neurobiol 2012;98:250-264.

Kim W, Miller JW, Ojemann JG, Miller KJ. Ictal localization by invasive recording of infraslow activity with DC-coupled amplifiers. J Clin Neurophysiol 2009;26:135-144.

Kuffler SW, Nicholls JG, Orkand RK. Physiological properties of glial cells in the central nervous system of amphibia. J Neurophysiol 1966;29:768-787.

Lapilover EG, Lippmann K, Salar S, Maslarova A, Dreier JP, Heinemann U, et al. Peri-infarct blood-brain barrier dysfunction facilitates induction of spreading depolarization associated with epileptiform discharges. Neurobiol Dis 2012;48:495-506.

Le Van Quyen M, Bragin A. Analysis of dynamic brain oscillations: methodological advances. Trends Neurosci 2007;30:365-373.

Koubeissi M. Subdural electrodes. In: Lüders H, editor. Textbook of epilepsy surgery. London: Informa, 2008:641-648.

MacFarlane SN, Sontheimer H. Electrophysiological changes that accompany reactive gliosis in vitro. J Neurosci 1997;17:7316-7329.

Mader EC, Jr., Fisch BJ, Carey ME, Villemarette-Pittman NR. Ictal onset slow potential shifts recorded with hippocampal depth electrodes. Neurol Clin Neurophysiol 2005;2005:4.

Matsumoto R, Nair DR, LaPresto E, Najm I, Bingaman W, Shibasaki H, et al. Functional connectivity in the human language system: a cortico-cortical evoked potential study. Brain 2004;127:2316-2330.

Modur PN, Scherg M. Intracranial broadband EEG analysis and surgical outcome: case report. Clin Neurophysiol 2009;120:1220-1224.

Modur PN, Zhang S, Vitaz TW. Ictal high-frequency oscillations in neocortical epilepsy: implications for seizure localization and surgical resection. Epilepsia 2011;52:1792-1801.

Modur PN, Vitaz TW, Zhang S. Seizure localization using broadband EEG: comparison of conventional frequency activity, high-frequency oscillations, and infraslow activity. J Clin Neurophysiol 2012;29:309-319.

Nariai H, Matsuzaki N, Juhasz C, Nagasawa T, Sood S, Chugani HT, et al. Ictal high-frequency oscillations at 80-200 Hz coupled with delta phase in epileptic spasms.

Epilepsia 2011a;52:e130-134.

Nariai H, Nagasawa T, Juhasz C, Sood S, Chugani HT, Asano E. Statistical mapping of ictal high-frequency oscillations in epileptic spasms. Epilepsia 2011b;52:63-74.

Ochi A, Otsubo H, Donner EJ, Elliott I, Iwata R, Funaki T, et al. Dynamic changes of ictal high-frequency oscillations in neocortical epilepsy: using multiple band frequency analysis. Epilepsia 2007;48:286-296.

Parri HR, Gould TM, Crunelli V. Spontaneous astrocytic Ca2+ oscillations in situ drive NMDAR-mediated neuronal excitation. Nat Neurosci 2001;4:803-812.

Rampp S, Stefan H. Ictal onset baseline shifts and infraslow activity. J Clin Neurophysiol 2012;29:291-297.

Ren L, Terada K, Baba K, Usui N, Umeoka S, Usui K, et al. Ictal very low frequency oscillation in human epilepsy patients. Ann Neurol 2011;69:201-206.

Rodin E, Constantino T, van Orman C, Funke M, Devinsky O, Wong P, et al. Optimal evaluation of digital electroencephalograms. Clin EEG Neurosci 2006;37:178-189.

Rodin E, Constantino T, van Orman C, House P. EEG infraslow activity in absence and partial seizures. Clin EEG Neurosci 2008a;39:12-19.

Rodin E, Modur P. Ictal intracranial infraslow EEG activity. Clin Neurophysiol 2008b;119:2188-2200.

Rodin E, Constantino T, Rampp S, Modur P. Seizure onset determination. J Clin Neurophysiol 2009;26:1-12.

Rodin E, Constantino T, Bigelow J. Interictal infraslow activity in patients with epilepsy. Clin Neurophysiol 2013 (In press. DOI:10.1016/j.clinph.2013.10.014).

Shih JJ, Rodin E, Gupta V, Wharen RE. Signal characteristics of intraventricular electrodes recordings in human epilepsy: a case report. Clin EEG Neurosci 2012;43:105-111.

Speckmann E, Elger C. Introduction to the Neurophysiological Basis of the EEG and DC Potentials. In: Niedermeyer E, Lopes da Silva F, editors. Electroencephalography: Basic principles, clinical applications and related fields fourth edition ed. Baltimore: Williams & Wilkins, 1999:15-27.

Thordstein M, Lofgren N, Flisberg A, Bagenholm R, Lindecrantz K, Kjellmer I. Infraslow EEG activity in burst periods from post asphyctic full term neonates. Clin Neurophysiol 2005;116:1501-1506.

Tian GF, Azmi H, Takano T, Xu Q, Peng W, Lin J, et al. An astrocytic basis of epilepsy. Nat Med 2005;11:973-981.

Worrell GA, Gardner AB, Stead SM, Hu S, Goerss S, Cascino GJ, et al. High-frequency oscillations in human temporal lobe: simultaneous microwire and clinical

macroelectrode recordings. Brain 2008;131:928-937.

Wu S, Kunhi Veedu HP, Lhatoo SD, Koubeissi MZ, Miller JP, Luders HO. Role of ictal baseline shifts and ictal high-frequency oscillations in stereo-electroencephalography analysis of mesial temporal lobe seizures. Epilepsia 2014.

Ylinen A, Bragin A, Nadasdy Z, Jando G, Szabo I, Sik A, et al. Sharp wave-associated high-frequency oscillation (200 Hz) in the intact hippocampus: network and intracellular mechanisms. J Neurosci 1995;15:30-46.

Figure Legends:

Figure 1: Subjects.

Figure 2: Ictal DC shift and HFO definition. The upper panel shows spectrogram, ictal DC shift waveform, and conventional ictal change in Patient 8. A part of the epoch is shown in the lower panel. Spectrograms: Vertical frequency range=1-300 Hz, frequency resolution=10 Hz, time resolution=100 ms. Calibration bars: vertical=1000 μV and horizontal=5 seconds in the upper panel, and vertical=1000 μV and horizontal=1 second in the lower panel. HFF=high frequency filter.

Figure 3: Electrode selection in Patient 14 (low grade neuroepithelial tumor). The upper 2 panels show ictal DC shifts for all electrodes implanted in 2 different seizures. The lower panel shows HFOs for all electrodes implanted in 1 seizure. Red vertical line indicates conventional initial change. Ictal DC shifts were observed reproducibly at 2 relatively restricted, but separate groups of electrodes (navy ovals). HFOs were distributed more diffusely (yellow arrows). In this patient, A1 and F6 electrodes (purple arrows in upper 2 panels) were selected for ictal DC shifts, and C2, F6 electrodes

(purple arrows in the lower panel) for HFOs based on the criteria described in the text. The upper panels: HFF 1 Hz. Calibration bars: vertical=1000 μV, horizontal=5 seconds. The lower panel: Vertical frequency range of the spectrograms=1-500 Hz. Horizontal calibration bar=5 seconds. Frequency resolution=10 Hz, time resolution=100 ms. Color coordinate: logarithmic scale (-3 to 3). HFF=high frequency filter.

Figure 4: Patient 3 with no conventional ictal change. A mass lesion (light blue arrows) was shown in magnetic resonance imaging (DIR: double inversion recovery). The lesion had calcification (CT: computer tomography). Subdural electrodes were implanted in the right mesial frontal and parietal lobes over the lesion. Ictal DC shifts (navy ovals) and HFOs (yellow arrows) were recorded with reproducibility. Ictal DC shift wave forms: HFF 1 Hz. Spectrograms: Vertical frequency range=1-500 Hz, frequency resolution=10 Hz, time resolution=100 ms. Calibration bars: vertical=500 μV, horizontal=5 seconds. HFF=high frequency filter.

Figure 5: Onset times of ictal DC shifts and HFOs relative to conventional change, which is set to time 0. Red is ictal DC shifts, and black HFOs. Patient 3 showed no conventional ictal change, and ictal DC shift onsets are plotted relative to HFO onsets,

which are set to time 0. Ictal DC shifts tended to occur earlier than HFOs. In 5 out of 7 patients with both ictal DC shifts and HFOs, the onset difference was statistically significant (Patient 4, 7, 9: Student's t test, $p<0.05$. Patient 8, 14: Wilcoxon rank sum test, $p<0.05$).

Figure 6: Patient 14 showed ictal DC shifts (navy oval) at a depth electrode (A1) in the white matter. The upper panel shows, from the top to the bottom, spectrogram, ictal DC shift waveform, and conventional ictal change for A1. The spectrogram shows no apparent HFOs. Spectrogram: Vertical frequency range=1-500 Hz, frequency resolution=10 Hz, time resolution=100 ms. Calibration bars: vertical=500 μV and horizontal=5 seconds. Ictal DC shift wave forms: HFF 1 Hz. HFF=high frequency filter. The lower panel shows location of the electrode [T1-weighted image. Left: Axial image showing A1 electrode as black signal defects within the broken circle. Location of the tumor is indicated with arrow heads. Right: Oblique image from anterior-right to posterior-left along a dimension indicated with a white line in the left panel. A1-4 depth electrodes are appreciated as black signal defects. A1 electrode is marked with an arrow. AR=anterior-right; PL=posterior-left; R=right; L=left.

Table 1: Summary of each patient

PATIENT	AGE AT ONSET	AGE AT SURGERY	SEX	CLINICAL EPILEPSY DIAGNOSIS	SZ TYPE	SZ SEMIOLOGY	SCALP EEG	MRI	FDG-PET	ICTAL SPECT	SURGERY	ELECTRODE PLACEMENT	PATHOLOGY	OUTCOME	SZ ANALYZED (TOTAL)
1	40y	40y	M	L FP	CPS	motor	intermittent slow L hemi	mass lesion at L FP	↑ L FP	not done	TR	L F/P	mixed oligoastrocyotoma	I	10(46)
2	29y	34y	M	L F	SPS/sGTCS	motor	epileptic discharge -	mass lesion at L F	not done	not done	TR	L F/P	anaplastic oligoastrocytoma	I	4(8)
3	11y	44y	M	R F	SPS	motor	intermittent slow L or R hemi	mass lesion at R F	↓ R F	R F	TR+ES	R F/P	mixed oligoastrocytoma/FCD IA	I	10(142)
4	12y	20y	F	R T	SPS/CPS	aura→CI	SZ pattern L and/or R T	mass lesion at R T	↓ R T	not done	TR+ES	R F/T	oligodendroglioma/FCD IB-IIA	I	10(73)
5	16y	22y	M	L FT	SPS/CPS/sGTCS	dyspnea	SZ pattern bilateral Fp or F	cortical thickening & cortico-medullary blurring at L F	↓ L T	not done	ES	L F/T	gliosis/FCD IA	I	2*(18)
6	3y	23y	F	R F	CPS	hypermotor	sharp wave L or R T	WNL	↓ bil FT	R F/basal ganglia	ES	R F/T/P	FCD IA	I	2(2)
7	10y	24y	M	L F	CPS	automotor	SZ L T	WNL	WNL	not done	ES	L F/T/P	FCD IB	I	9(29)
8	15y	32y	F	L TP	CPS	CI	SZ pattern L T	WNL	WNL	cluster of area-	ES	L F/T/P	FCD IA-IIA	I	10*(16)
9	10m	27y	M	R TP	SPS/sGTCS	negative myoclonus	spike R P	HIA, cortico-medullary blurring & abnormal sulcus at R P/post R MTL resectio	↓ R hemi	not done	ES	R F/P/O	FCD IIA	IV	10(28)
10	16y	23y	M	R O	SPS/CPS	aura→automotor	SZ pattern bilateral pos quad	HIA high & atrophy at R O	↓ R O	not done	ES	R O	FCD IIA	I	3(3)
11	1w	27y	M	R TO	SPS/CPS	aura→CI	SZ pattern R pos quad	atrophy at R TPO	↓ R TPO	not done	ES	R T/O	FCD IIA-B	II	2(3)
12	11y	17y	F	L T	CPS	CI	SZ pattern L T	laminar blurring at L hippocampus/arachnoid cyst at L T tip	↓ L T	not done	ES	L F/T/P	FCD IB	I	5(437)
13	8y	38y	F	L T	SPS/CPS/sGTCS	aura→automotor	SZ pattern L T	L HS	↓ L T	not done	ES	L F/T/P	FCD IIA	I	4*(5)
14	24y	28y	F	R P	CPS/sGTCS	automotor	SZ pattern R and/or L T, or R FC	mass lesion at R P	↓ R P	not done	TR+ES	R F/P	low grade neuroepithelial tumor	I	10(43)
15	7-8y	29y	M	L T	SPS/CPS	automotor	SZ pattern L T	atrophy at L T/T2WI high & small size of L hippocampus	↓ L T	not done	ES	L F/T/P	HS/mild dysplastic change	I	7*(8)
16	8y	34y	M	R TP	SPS/CPS	automotor	SZ pattern R FC and/or T	old traumatic change at R P/small size of bilateral hippocampus	↓ R TP	not done	ES	R F/T/P	FCD IA/HS	1	10*(13)

Abbreviations: C = central; CI = consciousness impairment; CPS = complex partial seizure; EEG = electroencephalography; ES = epilepsy surgery; F = 'female' in 'SEX' column/'frontal' in the other columns; FCD = focal cortical dysplasia;
FDG-PET = 18F-fluorodeoxyglucose-positron emission tomography; hemi = hemisphere; Fp = frontopolar; HIA = high intensity area in T2 weighted image and/or fluid-attenuated inversion recovery image; HS = hippocampal sclerosis; L = left; M = male;
m = month; MRI = magnetic resonance imaging; MTL = mesial temporal lobe; O = occipital; P = parietal; pos: posterior; quad = quadrant; R = right; sGTCS secondary generalized tonic clonic seizure; SPECT = single photon emission computed tomography;
SPS = simple partial seizure; SZ = seizure; T = temporal; TR = tumor resection; w = week; y = year, WNL = within normal limits

Simbols: ↑ = increased uptake; ↓ = decreased uptake

FCD classification is based on Palmini et al., 2004.

Outcome is based on Engel classification (Engel et al., 1993)

*Sampling rate: 1000 Hz

Table 2: Ictal DC shift/HFO occurrence rates

PATIENT	SEIZURES WITH DC SHIFTS OR HFO/SEIZURES ANALYZED (%)		CONVENTIONAL
	DC SHIFTS	HFO	EEG CHANGE
1	9/10 (90%)	0/10 (0%)	+
2	0/4 (0%)	0/4 (0%)	+
3	10/10 (100%)	9/10 (90.0%)	-
4	10/10 (100%)	10/10 (100%)	+
5	2/2 (100%)	2/2 (100%)	+
6	0/2 (0%)	0/2 (0%)	+
7	6/9 (66.7%)	3/9 (33.3%)	+
8	10/10 (100%)	10/10 (100%)	+
9	9/10 (90%)	4/10 (40%)	+
10	3/3 (100%)	0/3 (0%)	+
11	0/2 (0%)	0/2 (0%)	+
12	4/5 (80.0%)	0/5 (0%)	+
13	2/4 (50.0%)	0/4 (0%)	+
14	10/10 (100%)	10/10 (100%)	+
15	0/7 (0%)	2/7 (28.6%)	+
16	2/10 (20.0%)	0/10 (0%)	+

Abbreviations: DC = direct current; EEG = electroencephalography; HFO = high frequency oscillations

Symbols: + = present; - = absent

Table 3: Electrodes with ictal conventional electrocorticographic, DC and HFO changes

PATIENT	NUMBER OF ELECTRODES DC**		CONVENTIONAL		HFO***	NUMBER OF ELECTRODES WITH BOTH ICTAL DC SHIFTS AND HFO (%)
1	9*	<	11		-	
4	2*	<	3		6*	2 (33.3)
5	6*		2*		3*	3 (50.0)
7	2*	<	28	>	15*	1 (6.3)
8	27*		22	>	19*	23 (82.1)
9	36*	<	54	>	5*	5 (13.9)
10	1*	<	5		-	
12	3*		1*		-	
13	4*	<	12*		-	
14	6*	<	14		23*	3 (11.5)
15	-		2*		2*	
16	3*	<	42		-	
3****						2 (40.0)

Abbreviations:
CONVENTIONAL = conventional electroencephalogram
DC = direct current shifts
HFO = high frequency oscillations

*Core electrodes less than 2 were identifiable for Conventional, DC or HFO.

**Electrodes with ictal DC shifts in at least two of the analyzed seizures were counted.

***Electrodes with HFOs in at least one of the analyzed seizures were counted.

****Patient 3 did not show conventional ictal EEG pattern, and numbers of electrodes with ictal DC shifts and HFOs were not compared to those with conventional ictal EEG pattern.

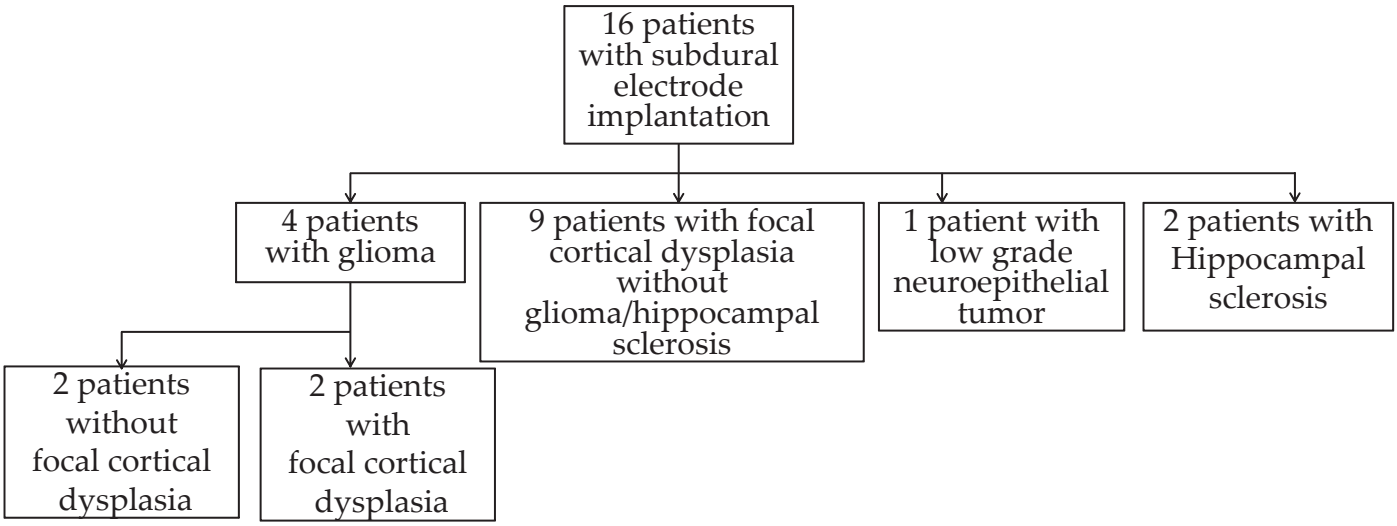
16 patients with subdural electrode implantation
4 patients with glioma
9 patients with focal cortical dysplasia without glioma/hippocampal sclerosis
1 patient with low grade neuroepithelial tumor
2 patients with Hippocampal sclerosis
2 patients without focal cortical dysplasia
2 patients with focal cortical dysplasia

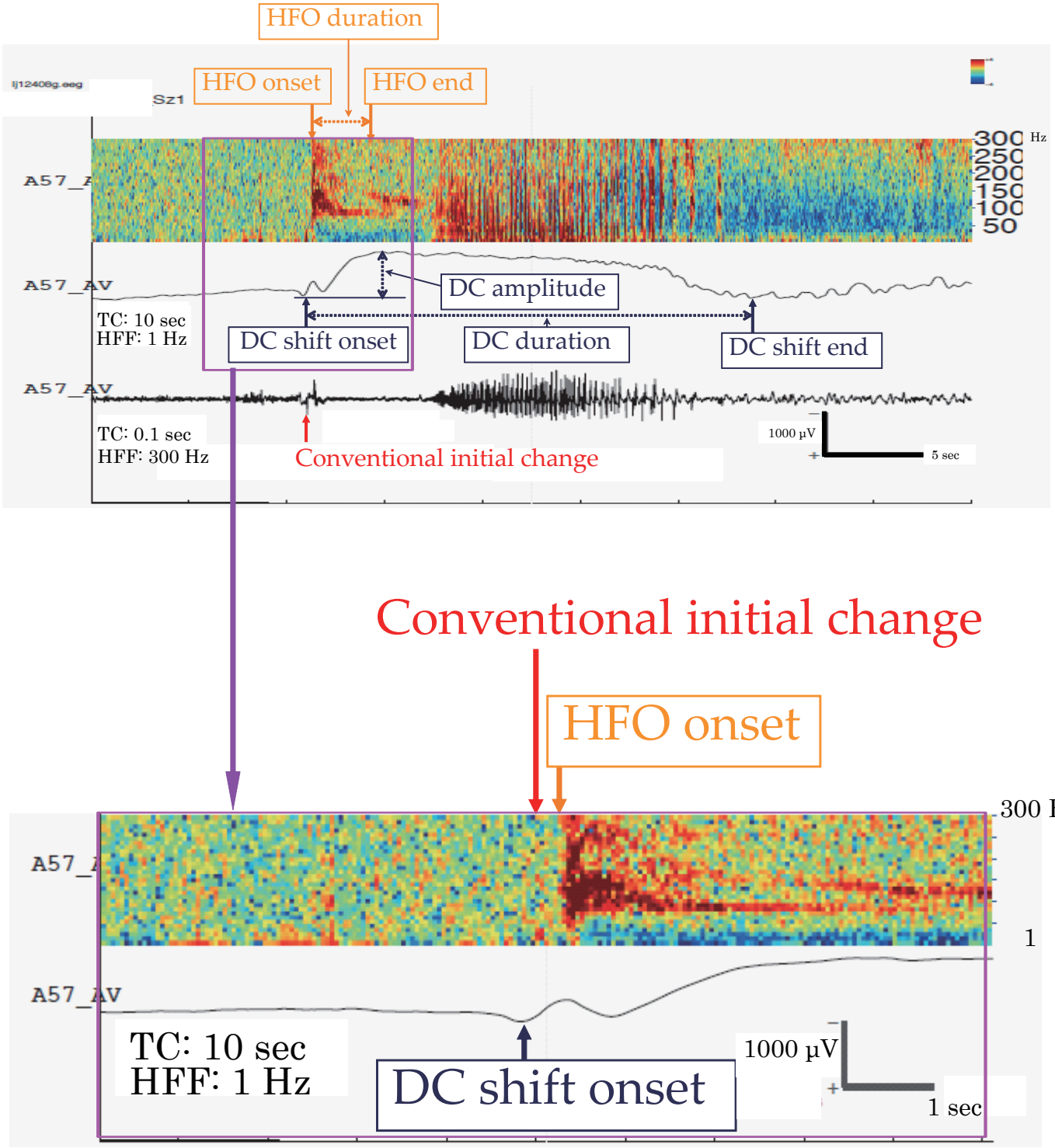
HFO duration
HFO onset
HFO end
Sz1
A57_A
A57_AV
300 Hz
250
200
150
100
50
DC amplitude
DC shift onset
DC duration
DC shift end
TC: 10 sec
HFF: 1 Hz
A57_AV
TC: 0.1 sec
HFF: 300 Hz
Conventional initial change
1000 µV
5 sec

Conventional initial change
HFO onset
300 Hz
A57_A
1
A57_AV
TC: 10 sec
HFF: 1 Hz
DC shift onset
1000 µV
1 sec

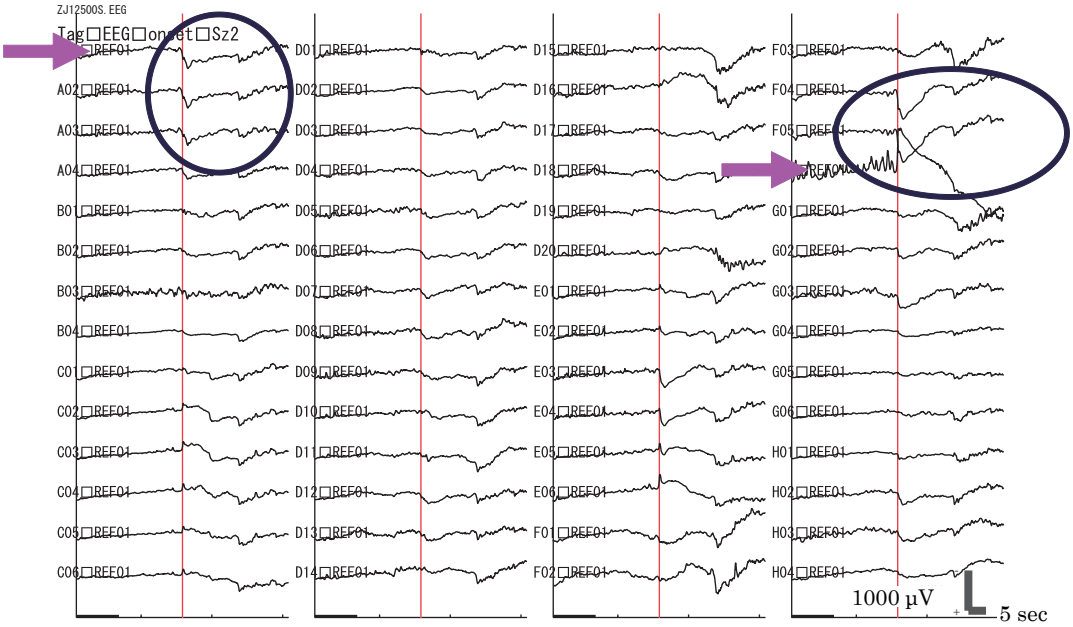

TC: 10 sec, HFF: 600 Hz

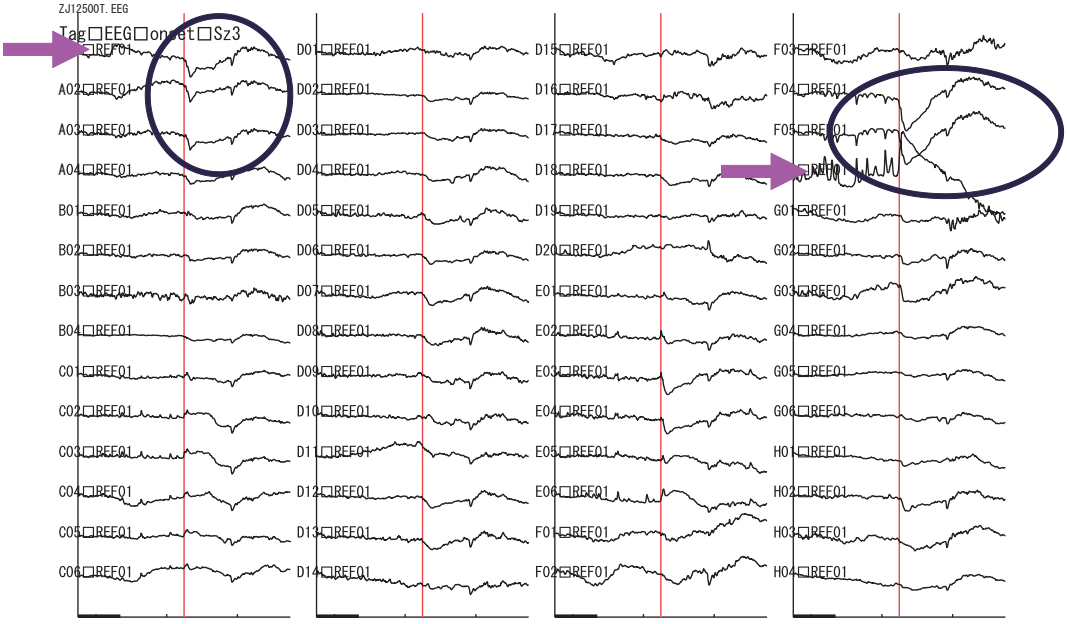

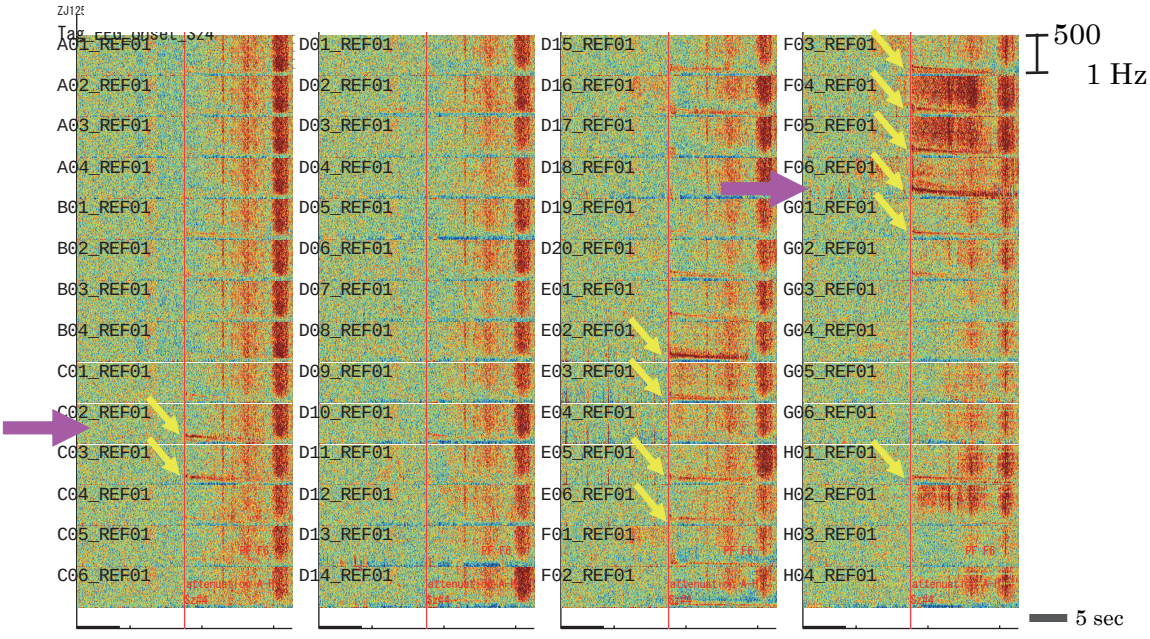

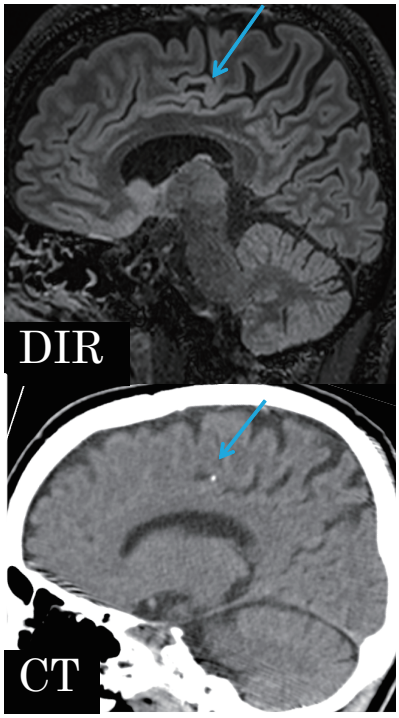
DIR
CT

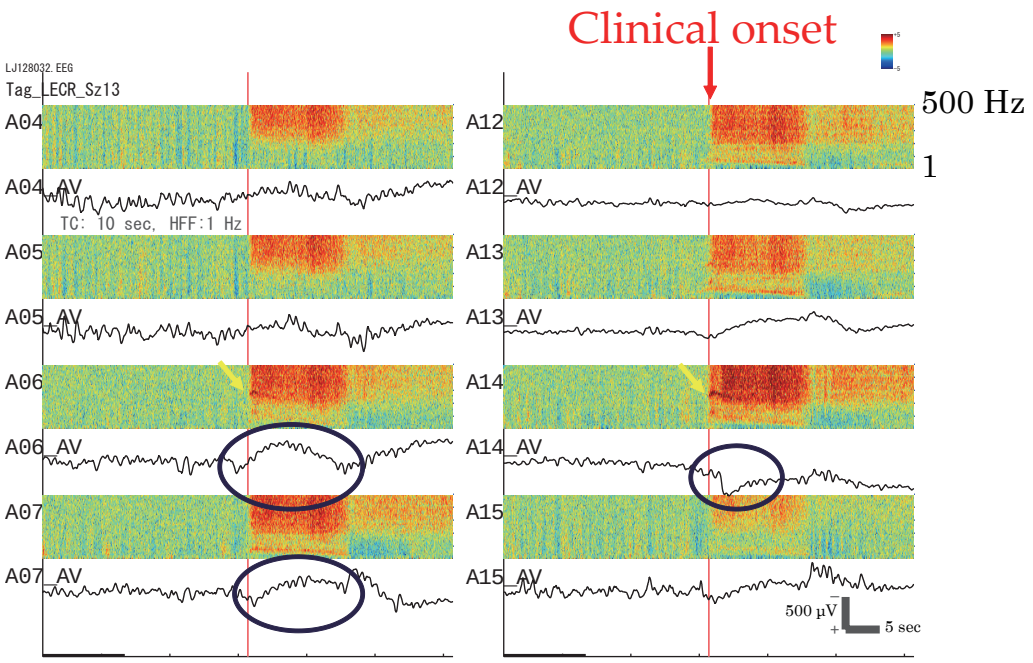
Clinical onset
LJ128032. EEG
Tag_ECR_Sz13
500 Hz
1
A04
A04_AV
TC: 10 sec, HFF:1 Hz
A05
A05_AV
A06
A06_AV
A07
A07_AV
A12
A12_AV
A13
A13_AV
A14
A14_AV
A15
A15_AV
500 μV
5 sec

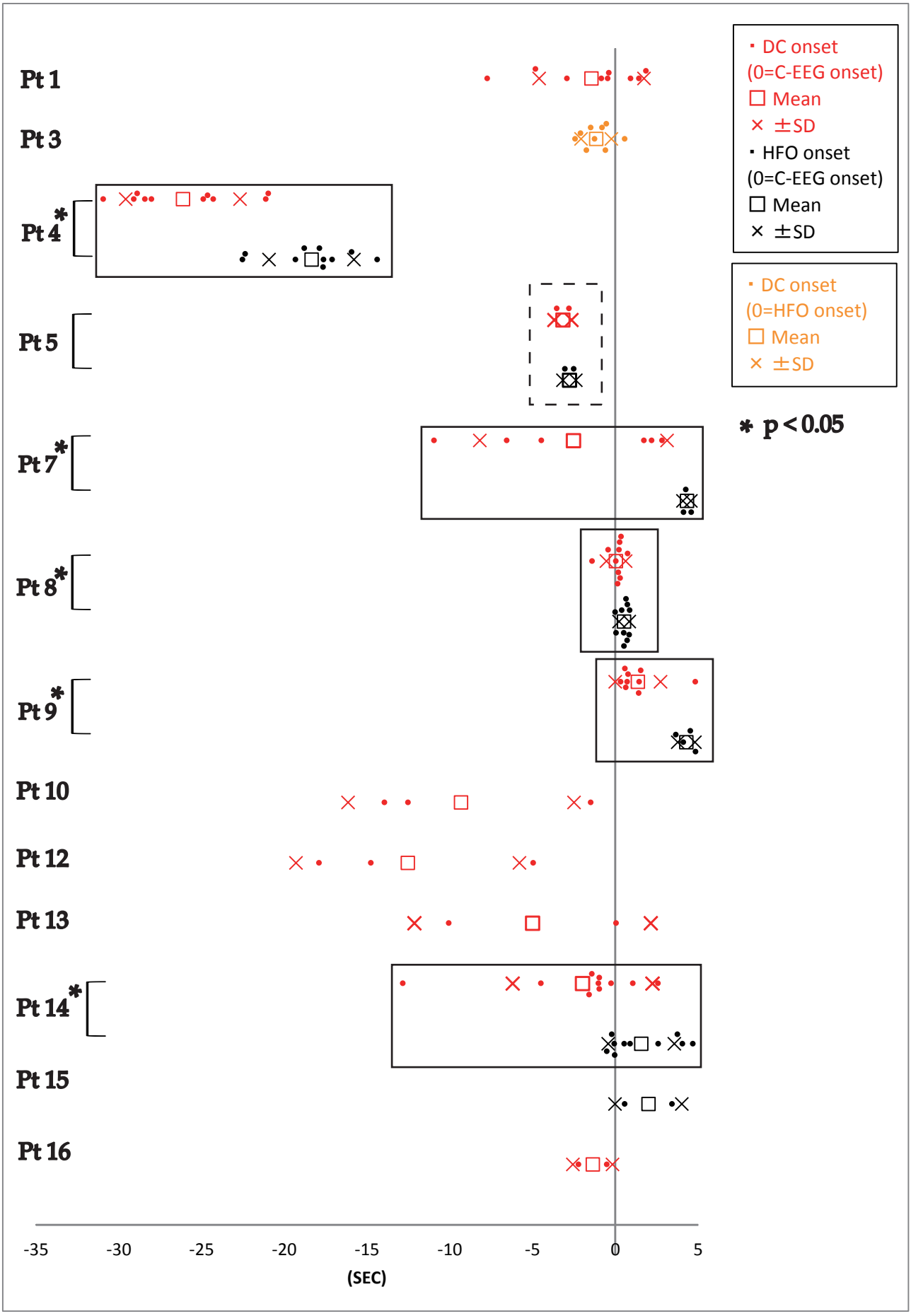
Pt 1
Pt 3
Pt 4*
Pt 5
Pt 7*
Pt 8*
Pt 9*
Pt 10
Pt 12
Pt 13
Pt 14*
Pt 15
Pt 16
-35
-30
-25
-20
-15
-10
-5
0
5
(SEC)
・DC onset
(0=C-EEG onset)
☐ Mean
× ±SD
・HFO onset
(0=C-EEG onset)
☐ Mean
× ±SD
・DC onset
(0=HFO onset)
☐ Mean
× ±SD
* p < 0.05

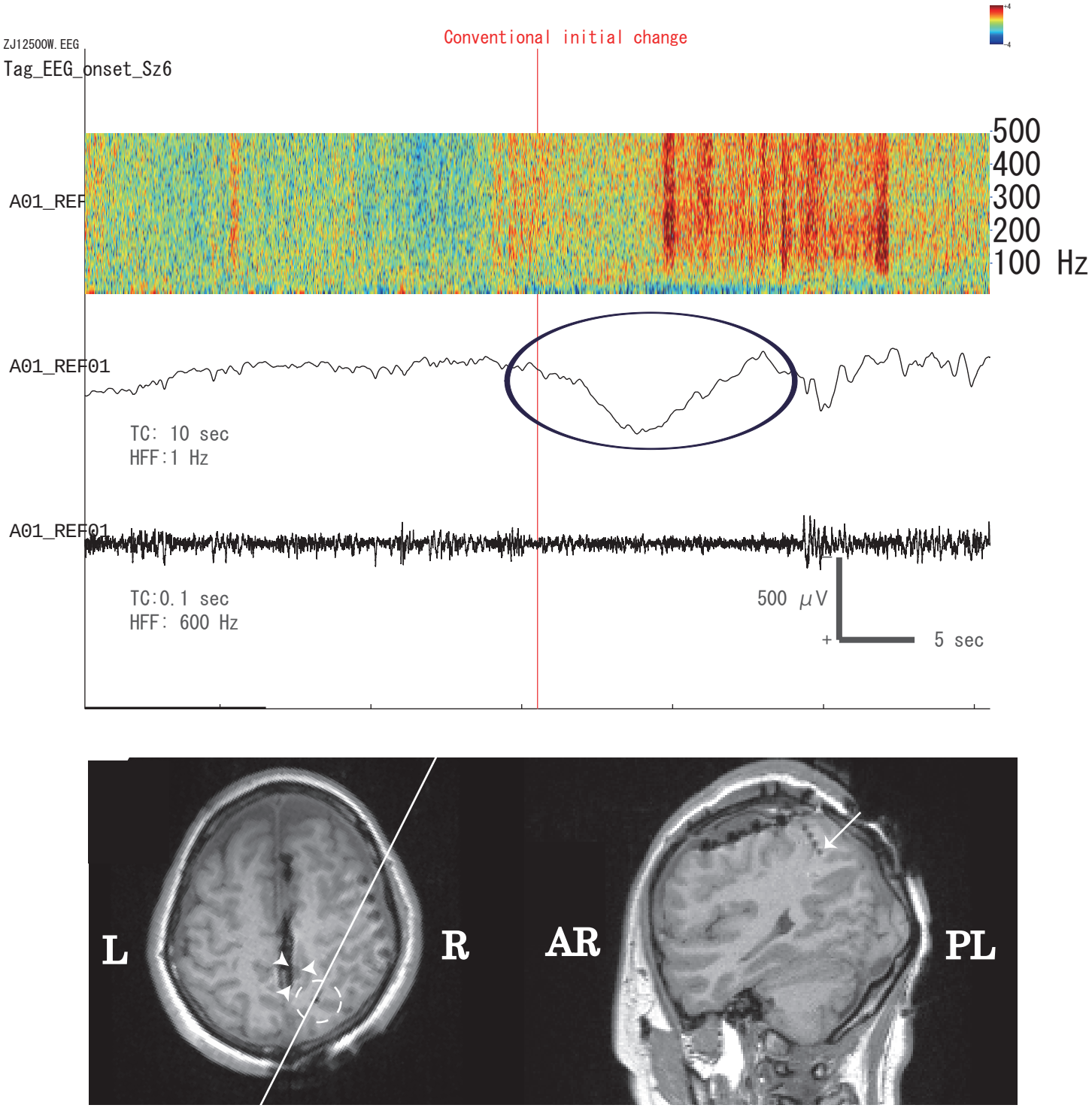
ZJ12500W.EEG
Conventional initial change
Tag_EEG_onset_Sz6
A01_REF
500
400
300
200
100 Hz
A01_REF01
TC: 10 sec
HFF:1 Hz
A01_REF01
TC:0.1 sec
HFF: 600 Hz
500 μV
5 sec

L
R
AR
PL